Finding the Specific Heat Capacity of Inverted Emulsions of Decane and Water

Elizabeth Fenstermacher

Institute for Nuclear Theory, University of Washington

Department of Physics, Mount Holyoke College

August 2003

Abstract

This paper examines the benefits of using Peltier AC Calorimetry to find the Specific Heat Capacity of Nanoliter portions of inverted monodisperse decane-water emulsions of differing droplet size. In doing so we investigate the role that interfacial energy, between the continuous and dispersed phase of an emulsion, plays in the processes of nucleation and melting.

1. Introduction

There is essentially no area of human activity that is not impacted, at least indirectly, by water. Despite the omnipresence of water and its importance to human activity there are still large gaps in our knowledge of the phase transitions that water undergoes. Two such processes that scienticists have been wrestling with for the last century are those of nucleation and melting.

In order to investigate these processes we have constructed a Peltier AC calorimeter with which to find the heat capacity of monodisperse inverted emulsions of decane and water over the range of $-30°C$ to $20°C$. In finding the heat capacity for a number of samples with different volume to surface area ratios we hope to be able to better understand what role interfacial energy between the continuous and dispersed phases plays for these processes.

1.1 Background

The simplest case of nucleation is that of homogenous nucleation or the spontaneous formation of the stable phase from the metastable phase. In the case of the water-ice systems we are interested in this would correspond to the formation of ice from supercooled water. In the homogenous case the obstacle to spontaneous nucleation is the high chemical potential at the surface of the nucleus. This high chemical potential is established by the loss of the entropic advantage without correspondingly gaining the stability of the nucleus. This entropic advantage is due to the rotational and translational freedom of molecules within in the liquid phase and the stability of the nucleus is due to being well-integrated into a crystal lattice. Since any nucleus initially formed will have a large surface area to volume ratio this high chemical potential will significantly inhibit the initial formation of the nucleus. Though the minimization of the Gibb's Free Energy by conversion of the metastable phase into the more thermodynamically stable phase will encourage nucleation the high chemical potential established by formation of the nucleus tends to prevent the process of nucleation until well below the freezing point causing supercooling. [9] In particular

$$\delta G(r) = \frac{-4\pi}{3} r^3 (\Delta\mu N_A v M) + 4\pi r^2 \gamma \qquad (1)$$

where r is the radius of the nucleus, $\delta\mu$ is the difference in chemical potential between the stable and metastable phases v is the volume of the solid, M is the molar weight, N_A is Avogadros number and γ is the interfacial energy [9]

Surface premelting before the melting supercooling. The high chemical to accomplish the phase random fluctuation the liquid phase. That is

The likelihood that nucleation will occur is dependent on the maximum Gibbs free energy fluctuation attainable along a certain pathway. The greater this maxiumum fluctuation is the more likely the energy for nucleation can be provided by random fluctuations withing the sample.

$$\delta G_{max} = \frac{16\pi\gamma_{SL}^3 v^2 T_m^2}{3q_{SL}^2 (T_m - T)^2} \qquad (2)$$

where q_{SL} is the late heat of fusion and T_m is the equilibrium melting temperature and $\gamma_{SL}4$ is the energy per unit area associated with the solid/liquid interface. [9]

Though it is necessary to have an understanding of homogenous nucleation before one can derive a

similar relationship for heterogenous nucleation, heterogenous nucleation is much more generalizable to real-world situations. In heterogenous nucleation the energetics and kinetics are profoundly altered by the presence of foreign materials. By introducing these foreign materials one is able to catalyze the process of nucleation. Ultimatlely we can derive the following expression that categorizes heterogenous nucleation in terms of the homogenous nucleation.

$$\delta G(r)^*_{het} = \delta G^*_{hom} f(\theta_{SL}) \tag{3}$$

where $f(\theta_{SL})$ is a geometric scaling factor only dependent on the contant angle of the nucleus [9]

$$f(\theta_{SL} = \frac{(2 + cos\theta_{SL})(1 - cos\theta_{SL})}{4} \tag{4}$$

This relationship demonstrates how nucleation becomes significantly more likely in the presence of foreign materials. This has been recognized empirically for decades, but there are still complications in understanding the exact process by which nucleation occurs. This empirically recognized relationship has led to such applications as cloud seeding. One material commonly used to catalyze the nucleation of supercooled water in clouds is silver iodide. Silver iodide is a crystalline structure whose lattice bears a resemblance to the lattice of water. This lent great credence to the initial proposal of epitaxial nuclation or the theory that heterogenous nucleation was the result of a crystalline substance serving as a substrate upon which ice could crystallize. Despite the widespread support epitaxial nucleation shared there were some serious flaws in the theory of epitaxial nucleation as initially proposed. One notable example being that barium fluoride a substance which also provides a good lattice fit upon which water could nucleate does not actually effectively catalyze the nulceation of water. These flaws eventually led to the abandonment of epitaxial nucleation as initially proposed; though work has been done recently that revisits the theory of epitaxial nucleation and has had promising results so far. This work considers the process with all the of thermodynamic parameters and as a two-dimensional phenomena. [9]

2. Experimental Set-up

In order to investigate the role that interfacial energy plays in these processes of nucleation and correspondingly melting we seek to find the heat capacity for an inverted emulsion of decane and water. Similar work has been done on emulsions in order to determine the C_p of the sample for the dynamic range of interest in our experiment. These earlier attempts though were made with differing experimental designs and we hope to improve upon this earlier work using our experimental design. [8]

2.1 Monodisperse Emulsions

We determined to use monodisperse emulsions because of the large surface area to volume ratio which allowed us to most efficiently study the effect of interfacial energy taking into account those factors already discussed as well as the Gibbs-Thompson effect. [**?**] This technique also has the added advantage of allowing us to treat and evaluate a large sample population prepared under identical conditions.

In order to generate the monodisperse emulsions that we used for this experiment we used a modification of a technique developed by Umbanhowar et al. This technique utilizes driven Rayleigh jet breakup in a coflowing system to produce droplets of a uniform size. Using this technique we are able to avoid drop recombination and coarsening and achieve a monodisperse emulsion. [4]

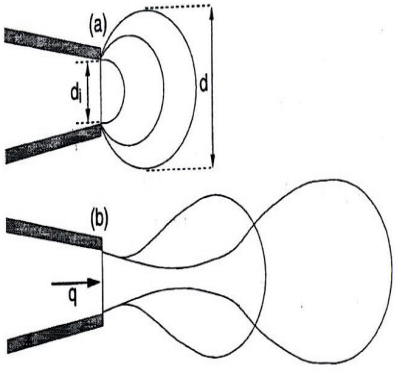

Figure 1 - Drop Break-off in a coflowing system [4].

In utilizing this method we constructed a mount for a 4.2 Watt Faulhaber motor ordered from micromotors incorporated which supported a teflon cup with a four inch inner diameter and a 1/4 inch lip. To this cup is added the continuous phase and the surfactant, in this case decane and Span-65. The cup is then spun at a constant angular velocity and the continuous phase quickly comes to equilibrium. Into the cup at a 45° angle is placed a glass capillary tube which has been treated to become hydrophobic. Water is then pumped through the capillary tube with a constant pressure after passing through a 0.1 μm filter and the drag from the coflowing system will create drops of fairly uniform size.

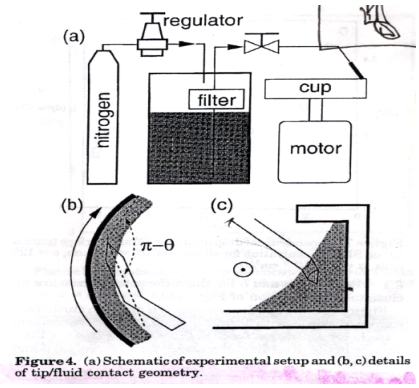

Figure 4. (a) Schematic of experimental setup and (b, c) details of tip/fluid contact geometry.

Figure 2- Set-up for generating emulsions. [4]

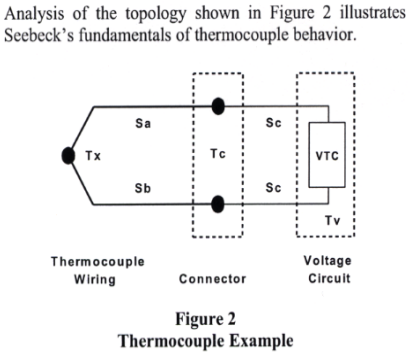

Figure 2
Thermocouple Example

Figure 3 - Basic Thermocouple Schematic http://www.dataforth.com/catalog/bb/190_1017231496.pdf

This emulsion was then examined underneath a video microscope to verify that we had indeed created an emulsion with a polydispersity low enough to be considered a monodisperse emulsion. This emulsion was then vacuum sealed in an aluminum cell.

2.2 Peltier AC calorimetry

Peltier AC Calorimetry is a modulated heating technique that uses thermocouples and the Peltier effect to alternatively heat and cool a sample. [1]

The Peltier effect is in its simplest form the result of the Seebeck effect and due to the fact that when a temperature difference exists across the length of a thermocouple, the end that is maintained at a higher temperature will be electron-deficient and the opposite end will become correspondingly electron-rich. By measuring the charge differential one is able to determine the temperature difference between the two ends. In order to establish an absolute temperature using the Peltier effect, one end of the thermocouple is maintained at a constant known temperature. [7]

In order to quantify the relationship we have established qualitatively we use Kirchoff's loop rule to find that

$$(S_a - S_b)(T_x - T_c) = [VTC] \tag{5}$$

here $(S_a - S_b)$ is a constant depending only on the two materials used and VTC is the voltage difference established between the two materials.

In order to utilize this effect to create modulated heating and cooling one controls the voltage potential established between the two materials. In the present one can establish the AC current oscillations. The junction with the sample with then alternatively act as a source or sink of heat and the pattern of heating and cooling will have been effectively established.

The great advantage of Peliter AC calorimetry is the elimination of the DC shift that is introduced in other modulated heating calorimetry techniques. As a result of this elimination the value of K_b is no longer constrained to be some arbitrarily large number to prevent the DC shift from becomining prohibitively large since $DC_{shift} = \frac{P_{DC}}{K_b}$ [1] In addition this eliminates the need for simultaneous temperature control of both the sample and the heat shield, since the temperature of the sample will osciallate around that of the heat shiled. [1]

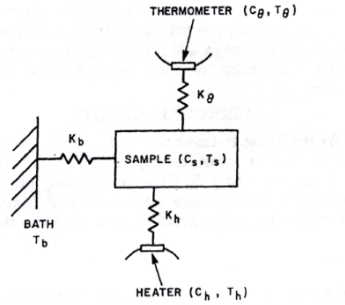

FIG. 1. Diagram of sample coupled to a bath, thermometer, and heater by the thermal conductances K_b, K_θ, and K_h, respectively.

Figure 4- schematic of AC calorimeter conductances where $K_b, K_\theta and K_h$ are the thermal conductances between the sample and the bath, thermometer and heater respectively [2]

If we consider the set-up of the calorimeter and using the definition of heat capacity we are able to write the following three equations. [2]

$$C_h \frac{T_h}{dt} = \frac{Q_h}{dt} = \frac{Q_0}{dt}(cos\frac{1}{2}\omega t)^2 - K_h(T_h - T_s), \tag{6}$$

$$C_s \frac{T_s}{dt} = \frac{Q_s}{dt}, \tag{7}$$

$$\frac{Q_s}{dt} = K_h(T_h - T_s) - K_b(T_s - T_b - K_\theta(T_s - T_\theta)), \tag{8}$$

$$C_\theta \frac{T_\theta}{dt} = \frac{Q_\theta}{dt} = K_\theta(T_h - T_\theta). \quad (9)$$

¿From this base set of equations one is able to derive the following expression.

$$\delta T_\omega = \frac{P_0}{\omega C_P}(1 + \frac{1}{\omega^2 \tau_{ext}^2} + \omega^2 \tau_{int}^2 + \frac{2K_b}{3K_s})^{\frac{-1}{2}} \quad (10)$$

Where ω refers to the frequency of the input AC current τ_{ext} refers to the time constant established between the sample and the heat bath and τ_{int} refers to the internal time constant of the sample.For a complete discussion of this derivation please refer to the work of Sullivan and Seidel. [2]

We now have an expression we can use to find C_p. As we noted earlier one of the unprecedented advantages of Peltier AC calorimetry is being able to make the value of K_b as small as experimental constraints allow. In this case K_b is simply due to the conduction of our 12 micron thick thermocouple and is therefore a vanishingly small quantity allowing us to eliminate the last term $\frac{2K_b}{3K_s}$ from our expression.

It is clear from the remaining expression

$$\delta T_\omega = \frac{P_0}{\omega C_P}(1 + \frac{1}{\omega^2 \tau_{ext}^2} + \omega^2 \tau_{int}^2)^{\frac{-1}{2}} \quad (11)$$

that if we choose ω appropriately then we can again greatly simplify this expression to the point where finding the value of C_p is trivial. We correspondingly choose a value of ω such that $\tau_{ext} >> \omega >> \tau_{int}$PAC

The expression then simplifies to

$$C_p = \frac{P_0}{\omega \delta T_\omega} \quad (12)$$

2.2.1 Peltier AC calorimeter design

The Peltier AC calorimeter used, consisted of a brass vacuum can Within which the can there were two thermocouples of constantan and chromel E both GE varnished onto the outside of the AL cell containing the emulsion. One thermocouple drives the AC oscillations and the other determines the temperature response of the sample. The sample cell with the thermocouples varnished to it is then GE varnished to a nylon washer on either side, which is suspended in the center of the vacuum can by means of an AL/SS mount. The thermocouple wires extend up through the top of the can through a thin-walled (approximately 6 thousandths of an inch) tube which is soldered into the top-plate of the brass can. The whole can is suspended above a liquid nitrogen bath and precisely temperature-controlled by means of a heating coil wound around the exterior of the can.

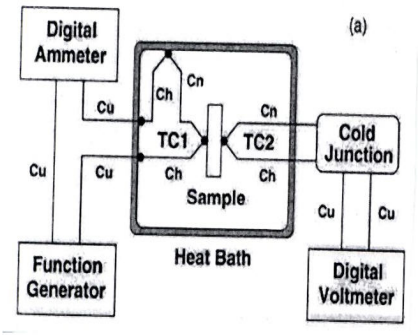

Figure 5 - Calorimeter Design [1]

2.2.2 Spot-Welding Thermocouples

In order produce thermocouples we used constantan and chromel E wire 50 microns thick. We then spot-welded these wires together using a spot-welder we constructed in accordance with the design of babic et al. [6] This spot welder was comprised of a copper block that acted as a ground and upon which the wires were aligned using Copper Berylium clips and a copper tip that was suspended above the block and attached to a circuit (see figure 6) which provided the current which created the weld.

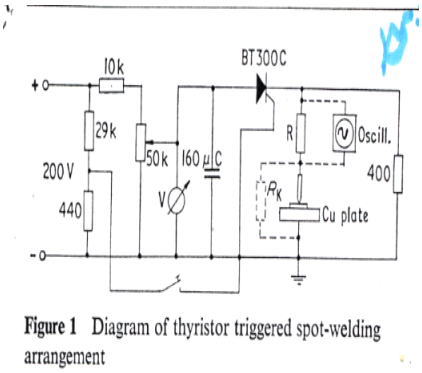

Figure 1 Diagram of thyristor triggered spot-welding arrangement

Figure 6- Circuit used in Spot Welder [6]

This current was released via a manual trigger and the current was set by use of a dial. In this way we produced all the thermocouples for the calorimeter.

3. Results and Conclusions

At the conclusion of the University of Washington's *Research Experience for Undergraduates* sponsored by the National Science Foundation for which this project was completed under the direction of Professor Gerald Seidler no heat capacity measurements had yet been made. The project will be continued by

Professor Gerald Seidler and University of Washington graduate student Adrianne Battle.

References

[1] Jung, D. H.; Moon, I. K.; Jeong, Y. H. *Thermochimica Acta* **2002** *391* 7.

[2] Sullivan, P. F.; Seidel, G. *Physicsal Review:* ***1968*** 173 679.

[3] Clause, D; Babin, L.; Broto, F.; Aguerd, M.; Clausse, M. *J. Phys. Chem*

[4] Umbanhowar "Monodisperse Emulsion Generation via Drop Break Off in a Coflowing Stream."

[5] Garfield, N. J.; Patel, M. *American Institute of Physics* **1998**, *69* 2186.

[6] Babic, E.; Leontic, B.; Vukelic, M. *Journal of Physics E. Scientific Instruments.* **1971**, *4* 382.

[7] Dataforth "Introduction to Thermocouples" http://www.dataforth.com/catalog/bb/190_1017231496.pdf

[8] Tombari, E.; Ferrari, C.; Salvetti, G; Johari, G. P. *American Institute of Physics* **1999**, emph111 3115.

[9] Seeley, L.H.; Seidler, G.T. In preparation.